Optical and Structural Characterization of Honeycomb-Like Ag$_2$S Nanoparticles by a Simplified and Stable Wet Chemical Synthesis Method

S.G. RUVALCABA-MANZO ⬤,[1,5] R. RAMÍREZ-BON,[2] J. TÁNORI,[3] R. OCHOA-LANDIN,[4] and S.J. CASTILLO[1]

1.—Departamento de Investigación en Física, Universidad de Sonora, Apdo. Postal 5-88, 83190 Hermosillo, Sonora, Mexico. 2.—Centro de Investigación y de Estudios Avanzados, IPN, Unidad Querétaro, Apdo. Postal 1-798, 76001 Querétaro, Querétaro, Mexico. 3.—Departamento de Investigación en Polímeros y Materiales, Universidad de Sonora, 83000 Hermosillo, Sonora, Mexico. 4.—Departamento de Física, Universidad de Sonora, Apdo. Postal 1626, 83000 Hermosillo, Sonora, Mexico. 5.—e-mail: manzosayra@gmail.com

The goal of this paper is to present a stable and new formulation route for the synthesis of silver sulfide nanoparticles with stoichiometric Ag$_2$S composition in aqueous solution. The structural, optical, and morphological properties of Ag$_2$S nanoparticles were studied by using characterization techniques such as ultraviolet–visible spectroscopy (UV–Vis), transmission electron microscopy and x-ray photoelectron spectroscopy (XPS). From the UV–Vis spectrum, the direct and indirect energy gap values of 3.56 and 1.89 eV were calculated, related to direct and indirect transitions of electrons, as an estimation of bandgaps. Also, an optical band gap shift with respect to bulk bandgap is observed reported in the literature and is related to nanoparticle size decrease. Furthermore, from the high-resolution transmission electron microscopy micrograph an orthorhombic crystallographic structure was determined with lattice parameters 4.77 × 6.92 × 6.88 Å and the nanoparticle surface showed a honeycomb-like interference pattern. Finally, the expected chemical composition was proved by the low- and high-resolution XPS spectra.

INTRODUCTION

Nowadays, the scientific community is interested in the development and study of materials at nanoscale due to the changes in the fundamental physical and chemical properties when decreasing the particle size in comparison to the same bulk material. Also, is known that the optical properties of nanoscale materials are closely related to the particle size, which is indicated by different colors due to the absorption phenomenon in the UV–visible region. Also, the main trend is searching for possible applications in many different areas of knowledge such as medicine, biology, and electronic devices. For example, cancer imaging,[1] detection of glucose, antibacterial activity,[2] photovoltaic cells[3] and near IR detectors.[4]

Nanostructured silver sulfide has been synthesized by various methods such as hydrochemical bath deposition,[5] sonochemical,[6] gamma-ray irradiation,[7] hydrothermal[8] and solvochemical,[9] obtaining different shapes and sizes of Ag$_2$S nanostructures by different synthesis methods. The bulk direct bandgap reported for Ag$_2$S is 1.3 eV.[10]

Sadovnikov,[11] reported nanoparticles of Ag$_2$S synthesized by the hydrochemical method with a range size from 500 nm to 60 nm and bandgap range of 0.96–1.21 eV, showing a potential antibacterial activity.

Optical and Structural Characterization of Honeycomb-Like Ag$_2$S Nanoparticles by a Simplified and Stable Wet Chemical Synthesis Method

2407

Kristl,[6] by ultrasonic irradiation, obtained strongly agglomerated Ag$_2$S nanoparticles with a direct bandgap of 4.5 eV by using ethylenediamine as the solvent and chelating agent, which requires special treatment because it releases irritating and toxic vapors.

Zhao[7] proposed a gamma-ray irradiation route at room temperature for the synthesis of Ag$_2$S nanorods with a monoclinic phase and a range size between 200 and 500 nm. There is a blueshift into the UV–Vis absorption spectrum and an increase in the direct bandgap, 2.34 eV, in comparison with bulk direct bandgap, 1.3 eV, of Ag$_2$S.

This research work deals with the optical, structural, and morphological study of the stable aqueous solution of Ag$_2$S nanoparticles from a wet chemical method at room temperature conditions. Additionally, we observed a bandgap shift with respect to bulk bandgap reported in the literature.

EXPERIMENTAL SECTION
Chemicals

Silver nitrate (AgNO$_3$, CAS:7761-88-8) was used as a metal source, thioacetamide (TAA, CAS: 62-55-5) as a chalcogen source and polyethyleneimine (PEI, CAS: 9002-98-6) as a complexing agent of the reaction. Aqueous solutions were prepared using deionized water.

Synthesis Procedure

The Ag$_2$S nanoparticles were obtained according to the wet chemical method are shown in Table I. The method consists of application of the first chemistry principles. The silver source utilized was the silver nitrate (AgNO$_3$), the polyethyleneimine (PEI) as a complexing agent which is necessary to modulate the reaction and thioacetamide (TAA) utilized as the metallic source for the obtention of sulfur ions. The reagents were prepared in aqueous solutions. Other important reaction conditions were to maintain the reaction at room temperature, stirring the reaction by ultrasonic vibration as well as working in an open atmosphere. To avoid the saturation of nanoparticles suspension was diluted in a mixture of water and acetone.

Table I. List of used compounds and the aggregation order to grow silver sulfide, Ag$_2$S, nanoparticles

Compound and order	Conc.	Volume
1. H$_2$O	–	2 mL
2. AgNO$_3$	0.1 M	0.15 mL
3. Polyethyleneimine (PEI)	xM	0.10 mL
4. Thioacetamide (TAA)	0.1 M	0.10 mL
5. H$_2$O	–	17 mL

Characterization

The optical characterization was obtained from a Genesis 10S UV–visible spectrophotometer. To characterize the morphology and crystalline phase of the Ag$_2$S sample we used transmission electron microscopy (TEM). XPS spectra were determined from a Phi 5100 spectrometer which is equipped with an ultra-high vacuum chamber of 2.79×10^{-10} kPa. The dual x-ray excitation source works in a range of energies from 0 to 1100 eV. The sample surface cleaning is argon ion beam at ultra-high vacuum conditions.

RESULTS
Optical Absorption

First, the absorption spectrum of Ag$_2$S is presented, in Fig. 1a and 1b as a function of wavelength and energy, respecitvely. As can be observed in Fig. 1a, the absorption is low between 400 and 900 nm, showing an absorption edge for wavelengths shorter than 370 nm. The absorption spectra behavior changes when it is a function of energy. Furthermore, an increasing absorption threshold related to the main electronic transitions is observed. The blueshift in the absorption edge is a consequence of the decrease of the nanostructure sizes, which is an indicator of energy gap increase. See Fig. 1b.

Figure 2 depicts the graphical methods to evaluate direct and indirect energy bandgaps. Generally, the bandgap refers to bulk semiconductors and the energy gap refers to nanoscale semiconductors. The
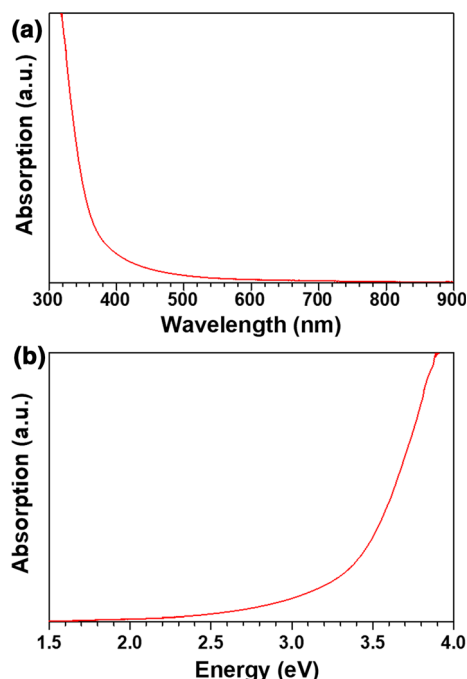

Fig. 1. (a) and (b) correspond to the absorption spectrum as a function of wavelength and energy, respectively
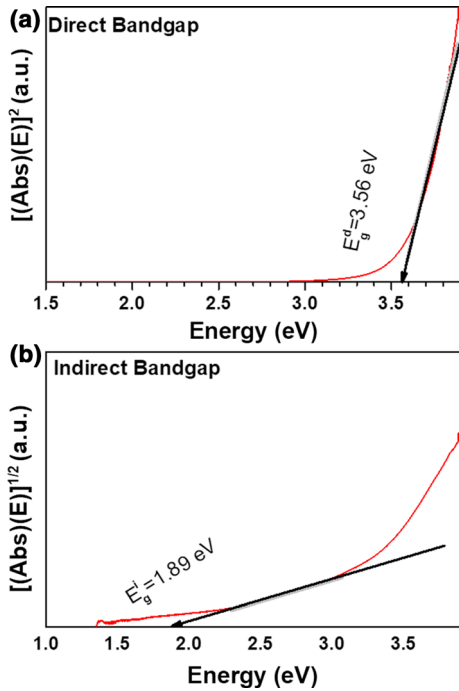
Fig. 2. (a) Direct and (b) indirect bandgap plots for silver sulfide, Ag_2S, nanoparticles calculated by a Tauc plot method

calculated energy gap values are 3.56 eV and 1.89 eV and correspond to (a) direct and (b) indirect transitions, respectively. The value of energy gap is greater than the bulk direct bandgap values reported for Ag_2S nanoparticles.[1,2]

Transmission Electron Microscopy

By using TEM and HR-TEM characterizations it was possible to observe a cluster of spherical-shaped nanoparticles on a working scale of 100 nm, as seen in Fig. 3a, and in Fig. 3b, by increasing the magnification of the scale work of 20 nm, we observed a set of spherical-shaped nanoparticles. A diameter of 14.82 nm, as indicated in Fig. 3c, corresponds to a single aleatory nanoparticle. Fast Fourier transform (FFT) and some interplanar distances of image Fig. 3c is shown in Fig. 3d. Finally, Fig. 3e is indicates the interplanar angle θ between the plane d3 and the plane d5.

The indices hkl were determined by comparison of experimental interplanar distances and interplanar distances reported in a crystallographic database PDF# 03-0844 for nanocrystalline orthorhombic silver sulfide and confirming a stoichiometry of Ag_2S (Table II).

According to Eq. (1) for *orthorhombic structure*, the interplanar angle θ between plane $(h_1k_1l_1)$ and plane $(h_2k_2l_2)$:

$$\theta = \cos^{-1}\left(\frac{\frac{h_1h_2}{a^2} + \frac{k_1k_2}{b^2} + \frac{l_1l_2}{c^2}}{\sqrt{\frac{h_1^2}{a^2} + \frac{k_1^2}{b^2} + \frac{l_1^2}{c^2}}\sqrt{\frac{h_2^2}{a^2} + \frac{k_2^2}{b^2} + \frac{l_2^2}{c^2}}}\right) \quad (1)$$

with $(h_1k_1l_1) = (004)$, $(h_2k_2l_2) = (120)$ and lattice parameters $a \times b \times c = 4.77 \times 6.92 \times 6.88$ and the following angle was found.

$$\theta = 90°$$

This was compared with the measured angle from Fig. 3e by ImageJ software.

The following results are in concordance with the HR-TEM results reported in this work. Also, Ibañez[12] proposed a colloidal synthesis method for PbS nanorods and tips of Ag_2S. The fast Fourier transform (FFT) of the HR-TEM image reveals an orthorhombic Ag_2S phase with cell parameters $a = 0.6725$ nm, $b = 0.4148$ nm, and $c = 0.7294$ nm. Additionally, Persson[13,14] developed an approximation of the Schrodinger equation for predicting the electronic structures of orthorhombic bulk Ag_2S and reported bulk bandgaps of 1.084 eV[13] and 1.296 eV.[14] Experimental and theoretical methods proposed by Santamaria-Perez[15] confirm a transition from a monoclinic phase to an orthorhombic phase for Ag_2S due to the decrease of pressure from 20.6 GPa to 5.4 GPa and then to a monoclinic phase at 10.6 GPa.

On the other hand, Sadovnikov[16] synthesized by chemical deposition and under monochromatic light irradiation with wavelength 450 nm, the Ag_2S/Ag hetero-nanostructure. The XRD pattern of the reported Ag_2S/Ag hetero-nanostructure contains two phases, the monoclinic α Ag_2S structure and metallic cubic silver Ag. A monoclinic crystal structure of Ag2S exists at temperatures below 450 K and the cubic phase exists in the temperature range 452–859 K. The high-temperature cubic phase of Ag2S is stable from 860 K up to melting point temperature. Also, Sadovnikov[17] synthesized non-stoichiometric nanopowders, $Ag_{1.93}S$, with a monoclinic acanthite-type structure and by hydrochemical deposition[18] synthesized Ag_2S nanoparticles with a monoclinic structure and cell parameters, $a = 0.42264$ nm, $b = 0.69282$ nm, $c = 0.95317$ nm and $b = 125.554$. Furthermore, Sadovnikov[19] reported the transformation of nanocrystalline Ag_2S with a monoclinic structure to cubic structure occurs as a result of electron beam heating at 450 K.

X-ray Photoelectron Spectroscopy (XPS)

The Ag_2S sample was dropped onto a glass slide for XPS analysis and the binding energies distribution were obtained, as shown in Fig. 4. The identified chemical elements in the sample by XPS analysis are C 1s, O 1s, Auger electrons C KVV, Auger electrons O KLL as environmental contaminants, N 1s from the residual compounds, and Si 2s and 2p attributed to the soda-lime glass substrate. Furthermore, were detected peaks concerning the main chemical elements forming our Ag_2S nanoparticles system, Ag 3p and 3d and S 2p. The binding
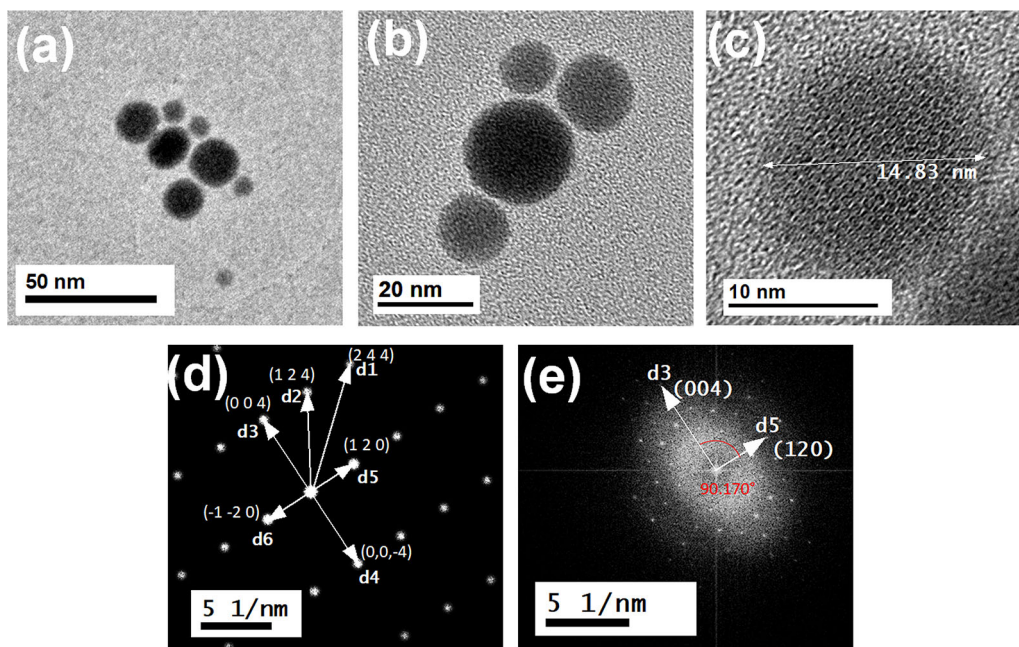
Fig. 3. TEM micrographs for (a) 100 nm and (b) 20 nm. (c) provides an HR-TEM micrograph of a single honeycomb-like Ag2S nanoparticle and (d) its corresponding fast Fourier transform (FFT). (e) verifiesthe angle between (004) and (120) planes

Table II. Comparison between the experimental and reported interplanar distances for orthorhombic Ag₂S nanoparticles and its corresponding Miller indices

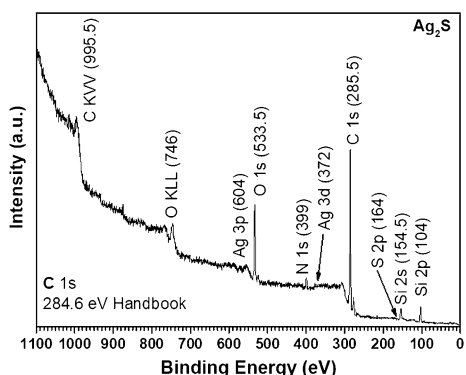| d_{hkl}	Exp. (Å)	Database (Å)	h	k	l
d1	1.085	–	2	4	4
d2	1.453	1.46	1	2	4
d3	1.705	1.72	0	0	4
d4	1.705	1.72	0	0	− 4
d5	2.805	2.81	1	2	0
d6	2.805	2.81	− 1	− 2	0

Fig. 4. XPS spectrum from 0 to 1100 eV region under low-energy resolution conditions for a silver sulfide, Ag₂S, sample

energies for each atomic sublevel are indicated in Fig. 4.

The main chemical composition of the Ag₂S sample was determined by high-resolution XPS
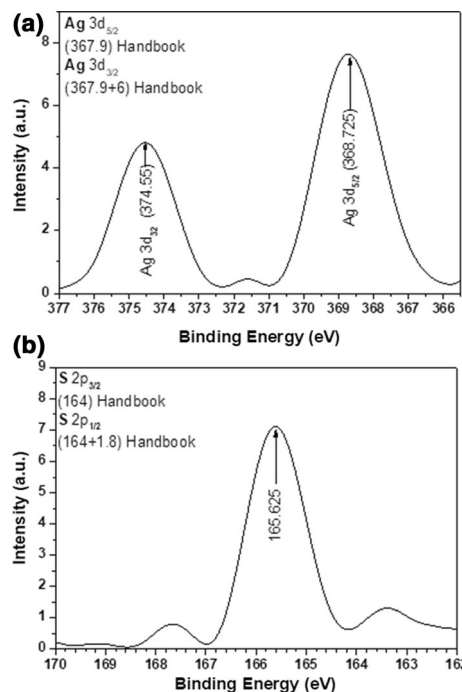

Fig. 5. XPS spectra for (a) silver and (b) under high-energy resolution conditions for a silver sulfide, Ag₂S, sample

analysis. First, by focusing on the carbon peak due to its calibration importance, it is well defined and located in the binding energy value of 285.825 eV, while typically it is located at 284.6 eV.[20] In Fig. 5a the energy difference of the electronic doublet of silver 3d is 5.825 eV, almost corresponding to the reported value of 6 eV.[21] However, the signal of

sulfur 2p behaves anomalously compared with the standard behavior reported as an electronic doublet, and the peak value location corresponds to a sulfite chemical compound, according to handbook XPS reference,[22] see Fig. 5b.

CONCLUSIONS

The obtained results in this research work are consistent with previously reported research in the literature. Stable Ag_2S nanoparticles were obtained in room temperature conditions by a wet chemical route of synthesis. The direct bandgap plot shows a large shift in energy in comparison to the direct bulk bandgap of 0.9–1.05 eV[23] for bulk Ag_2S and the direct bandgap of 1.76 eV[24] for Ag_2S nanoparticles. The direct and indirect bandgaps for Ag_2S are 3.56 eV and 1.89 eV, respectively. From TEM images was observed a spherical symmetry in nanoparticles and the HR-TEM micrograph provides the information to determinate an orthorhombic crystallinity structure for Ag_2S nanoparticles in comparison to reported monoclinic structure.[11,16–19] By XPS spectra was verify the presence of elements contained in the sample. The characterization techniques were enough to identify optically, structurally, and chemically the Ag_2S nanoparticles.

REFERENCES

1. H. Chen, B. Li, M. Zhang, K. Sun, Y. Wang, K. Peng, M. Ao, Y. Gou, and Y. Gu, *Nanoscale* 6, 12580 (2014).
2. Y. Delgado-Beleño, C.E. Martinez-Nuñez, M. Cortez-Valadez, N.S. Flores-López, and M. Flores-Acosta, *Mater. Res. Bull.* 95, 385 (2018). https://doi.org/10.1016/j.materresbull.2017.11.015.
3. U.M. Jadhav, S.N. Patel, and R.S. Patil, *Res. J. Chem. Sci.* 3, 69 (2013).
4. Y. Zhang and Q. Wang, *Mater. China* 35, 17 (2016). https://doi.org/10.7502/j.issn.1674-3962.2016.01.03.
5. A.I. Sadovnikov and S.I. Gusev, *J. Mater. Chem. A* 5, 17676 (2017).
6. M. Kristl, S. Gyergyek, and J. Kristl, *Mater. Express* 5, 359 (2015).
7. Y. Zhao, D. Zhang, W. Shi, and F. Wang, *Mater. Lett.* 61, 3232 (2007).
8. L. Lv and H. Wang, *Mater. Lett.* 121, 105 (2014). https://doi.org/10.1016/j.matlet.2014.01.121.
9. M.A. Karimi, M. Ranjbar, and A. Salmanipour, *J. Saudi Chem. Soc.* 21, 193 (2017).
10. S. Kashida, N. Watanabe, T. Hasegawa, H. Lida, M. Mori, and S. Savrasov, *Solid State Ion.* 158, 167 (2003).
11. S.I. Sadovnikov, Y.V. Kuznetsova, and A.A. Rempel, *Nano-Struct. Nano-Objects* 7, 251 (2016). https://doi.org/10.1016/j.nanoso.2016.06.004.
12. M. Ibáñez, A. Genç, R. Hasler, Y. Liu, O. Dobrozhan, O. Nazarenko, M. de la Mata, J. Arbiol, A. Cabot, and M.V. Kovalenko, *ACS Nano* 13, 6572 (2019).
13. K. Persson, Materials Data on Ag2S (SG:63) by Materials Project. United States. https://doi.org/10.17188/1207146.
14. K. Persson, Materials Data on Ag2S (SG:36) by Materials Project. United States. https://doi.org/10.17188/1206341.
15. D. Santamaría-Perez, M. Marques, R. Chulia-Jordan, J.M. Menendez, O. Gomis, J. Ruiz-Fuertes, J.A. Sans, D. Errandonea, and J.M. Recio, *Inorg. Chem.* 51, 5289 (2012).
16. S.I. Sadovnikov and A.I. Gusev, *Biointerface Res. Appl. Chem.* 6, 1797 (2016).
17. S.I. Sadovnikov, A.I. Gusev, and A.A. Rempel, *Phys. Chem. Chem. Phys.* 17, 12466 (2015).
18. S.I. Sadovnikov, A.I. Gusev, and A.A. Rempel, *Superlattices Microstruct.* 83, 35 (2015). https://doi.org/10.1016/j.spmi.2015.03.024.
19. S.I. Sadovnikov, A.I. Gusev, and A.A. Rempel, *Phys. Chem. Chem. Phys.* 17, 20495 (2015). https://doi.org/10.1039/c5cp02499d.
20. C.D. Wagner, W.M. Riggs, L.E. Davis, and J.F. Moulder, Carbon, in *Handbook of X Ray Photoelectron Spectroscopy: A Reference Book of Standard Spectra for Identification and Interpretation of Xps Data*, ed. G.E. Muilenberg (Eden Prairie: Physical Electronics, Inc., 1976), pp. 40–41.
21. C.D. Wagner, W.M. Riggs, L.E. Davis, and J.F. Moulder, Silver, in *Handbook of X Ray Photoelectron Spectroscopy: A Reference Book of Standard Spectra for Identification and Interpretation of Xps Data*, ed. G.E. Muilenberg (Eden Prairie: Physical Electronics, Inc., 1976), pp. 120–121.
22. C.D. Wagner, W.M. Riggs, L.E. Davis, and J.F. Moulder, Sulfur, in *Handbook of X Ray Photoelectron Spectroscopy: A Reference Book of Standard Spectra for Identification and Interpretation of Xps Data*, ed. G.E. Muilenberg (Eden Prairie: Physical Electronics, Inc., 1976), pp. 60–61.
23. R. Zamiri, H. Abbastabar Ahangar, A. Zakaria, G. Zamiri, and M. Shabani, *Chem. Cent. J.* 9, 28 (2015).
24. S.P. Anthony, *Mater. Lett.* 63, 773 (2009).